Yrast spectroscopy of $^{128}_{60}Nd_{68}$ and systematics of the $\nu h_{11/2}$ crossing in $A\sim130$ nuclei

O. Zeidan,* D. J. Hartley,† L. L. Riedinger, W. Reviol,‡ W. D. Weintraub,§ Y. Sun, and Jing-ye Zhang
Department of Physics and Astronomy, University of Tennessee, Knoxville, Tennessee 37996

A. Galindo-Uribarri and S. D. Paul‖
Physics Division, Oak Ridge National Laboratory, Oak Ridge, Tennessee 37831

D. G. Sarantites and M. Devlin¶
Chemistry Department, Washington University, St. Louis, Missouri 63130

M. P. Carpenter, R. V. F. Janssens, and D. Seweryniak
Physics Division, Argonne National Laboratory, Argonne, Illinois 60439
(Received 6 May 2002; published 29 October 2002)

High-spin states in ^{128}Ca were populated with the ^{92}Mo (^{40}Ca, $2p2n$) reaction at a beam energy of 184 MeV. The previously known ground-state band has been extended to $I^{\pi}=(34^{+})$ and four sidebands were observed. Configuration assignments for these sidebands are discussed based on their alignment behavior. A significant delay of the $\nu h_{11/2}$ crossing frequency is observed in the $A\sim130$ region, with the largest delays occurring consistently at $N=70$. Cranked shell model calculations were performed in order to investigate whether a variation of deformation and/or pairing parameters can account for this phenomenon.

DOI: 10.1103/PhysRevC.66.044311 PACS number(s): 21.10.Re, 23.20.Lv, 27.60.+j

I. INTRODUCTION

The region of nuclei with $Z\sim60$ and $N\sim70$ has been characterized by significant ground-state deformation ($\beta_2\sim0.3$) as the neutron Fermi surface is located near midshell ($N=66$) [1]. Shape coexistence has been observed in the region as highly deformed bands are found in several light $A\sim130$ nuclei [2–4]. In addition, these neutron-deficient nuclei provide an important means of testing the cranked shell model (CSM). The yrast structures of even-even nuclei near $A\sim130$ show evidence for the rotational alignment of an $h_{11/2}$ quasiproton pair at a well-defined rotational frequency in the range of $\hbar\omega=0.32-0.36$ MeV. This alignment is reproduced well by cranking calculations. In contrast, the alignment of $h_{11/2}$ quasineutrons generally occurs over a much wider range (0.5–0.7 MeV), and at a higher frequency than predicted by the CSM. Possible explanations for this surprising effect have been sought in the systematics of the lightest neodymium ($Z=60$), praseodymium ($Z=59$), and cerium ($Z=58$) isotopes. In the present work, we have investigated high-spin states in ^{128}Nd, the lightest Nd nucleus with known excited states, in order to study these alignment issues further. The extension of the ground-state sequence reveals that the $\nu h_{11/2}$ alignment is also significantly delayed in ^{128}Nd. However, no sensible combination of deformation and pairing parameters in the CSM calculations could reproduce this effect. In addition, four sidebands were observed and configurations were assigned, based on observed alignment behaviors and taking into account the quasiparticles located near the Fermi surface. It should be noted that a parallel work on this nucleus was also published [5] recently.

II. EXPERIMENTAL DETAILS

In an experiment emphasizing the population of some of the most neutron-deficient nuclei in the $A\sim130$ region, an 184-MeV ^{40}Ca beam from the ATLAS superconducting linear accelerator at Argonne National Laboratory (ANL) was delivered to a 0.625 mg/cm^2 thick, self-supporting ^{92}Mo target. Prompt γ rays were detected with 99 Compton-suppressed Ge spectrometers in the Gammasphere array [6]. Coincident charged particles were measured with the 95 CsI detectors of the Washington University Microball [7]. Approximately 116×10^6 fivefold (γ^5) or higher coincidence events were determined to have γ rays correlated with two-proton emission (comprising $\sim20\%$ of the total events). The γ rays were corrected for Doppler shifts and sorted into an $E_\gamma\times E_\gamma\times E_\gamma$ coincidence cube. The data analysis was performed with the RADWARE [8] software package and the level scheme for ^{128}Nd from the present data is shown in Fig. 1.

Relative spin assignments proposed for the states in ^{128}Nd were determined through directional correlation of oriented states (DCO) analysis. To facilitate this procedure, an

*Present address: Department of Radiation Oncology, Shands Cancer Center, University of Florida, Gainesville, FL 32610.
†Present address: Department of Physics, United States Naval Academy, Annapolis, MD 21402.
‡Present address: Chemistry Department, Washington University, St. Louis, MO 63130.
§Present address: Department of Physics, Florida State University, Tallahassee, FL 32306.
‖Present address: Department of Nuclear and Atomic Physics, Tata Institute of Fundamental Research, Mumbai 400 005, India.
¶Present address: Los Alamos National Laboratory, Los Alamos, NM 87545.

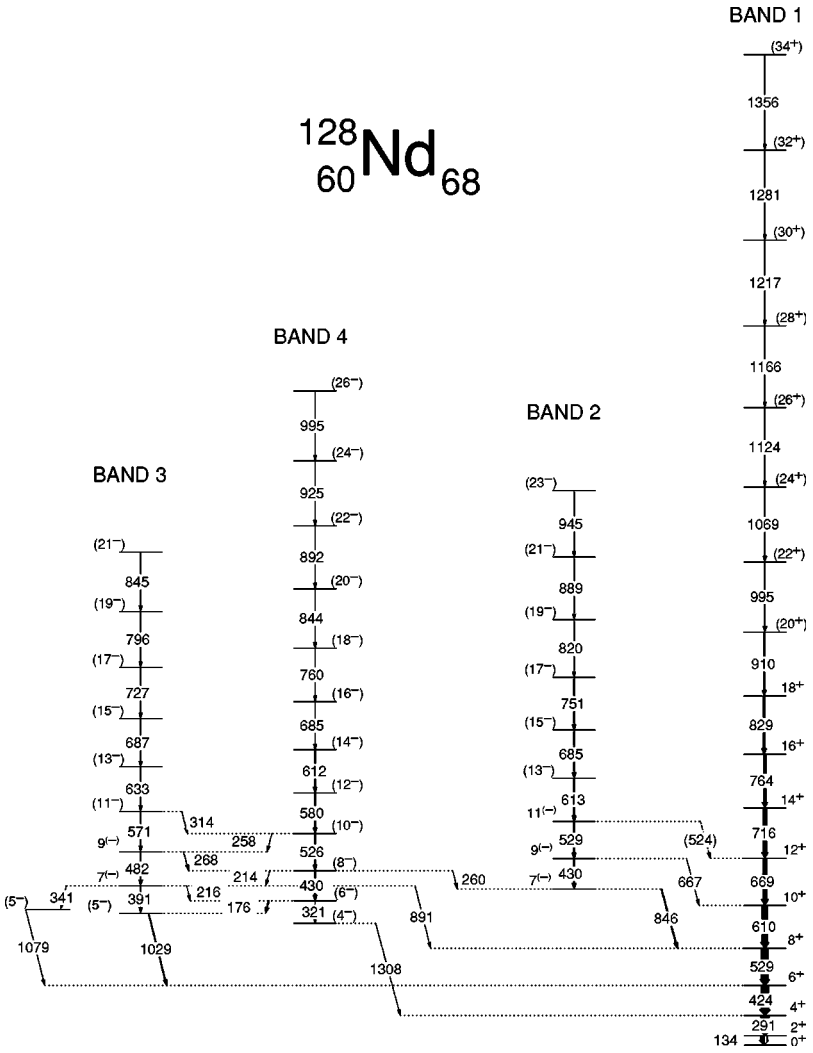

FIG. 1. The level scheme for ^{128}Nd. The width of the arrows is proportional to the intensity of the transition. Tentative transitions are denoted by dashed lines. Spin and parity assignments are explained in the text.

asymmetric coincidence matrix was created, where the energy of γ rays observed in detectors located at $\sim 35°$ and $\sim 145°$ were histogrammed along one axis and coincident γ rays observed in detectors located at $\sim 90°$ were histogrammed along the other. DCO ratios were determined from the expression

$$R_{DCO} = \frac{I_{\gamma_1}(\text{at } \sim 35° \text{or } \sim 145°; \text{in coincidence with } \gamma_2 \text{ at } 90°)}{I_{\gamma_1}(\text{at } 90°; \text{in coincidence with } \gamma_2 \text{ at } \sim 35° \text{ or } \sim 145°)},$$

where I_{γ_1} is the intensity of the γ ray of interest and γ_2 is a stretched $E2$ ($\Delta I = 2$) transition. With the detectors at the given angles, R_{DCO} values of approximately 0.5 are expected for pure dipole transitions ($M1$ and $E1$) and 1.0 for quadrupole transitions ($E2$). The measured DCO ratios are summarized in Table I along with the energy, spin, and parity of the states, as well as the energy and relative intensity of the depopulating γ rays. Weak transitions feeding states with determined spin values, for which a reliable DCO ratio could not be determined, were assigned a multipolarity by assuming that the rotational behavior of the sequence persists.

III. THE LEVEL SCHEME

Prior to our work, little was known about ^{128}Nd. The original identification of levels in the ground-state band was reported by Lister *et al.* [9] using γ-ray, charged-particle, and neutron detection techniques. Moscrop *et al.* [10] confirmed the ground-state band in ^{128}Nd up to $I^{\pi} = 14^{+}$. The present data enabled the extension of this sequence (labeled as band 1 in Fig. 1) by ten additional transitions to a maximum observed spin and parity of $I = (34^{+})$. A spectrum of the yrast structure is given in Fig. 2, which is a result of summing all coincidence spectra produced by double gating

TABLE I. Data for levels and γ rays in ^{128}Nd.

I_i^{π} [a]	E_{level} (keV)	E_γ (keV)[b]	I_γ	DCO[c]	Multipolarity
		Band 1			
2^+	133.7	133.7		0.93(7)	$E2$
4^+	425.0	291.3	$\equiv 100$	0.97(4)	$E2$
6^+	848.5	423.5	96(5)	0.99(4)	$E2$
8^+	1377.9	529.4	85(5)	0.93(4)	$E2$
10^+	1988.0	610.1	67(4)	0.94(9)	$E2$
12^+	2657.4	669.4	53(4)	0.88(4)	$E2$
14^+	3373.4	716.0	40(2)	0.91(5)	$E2$
16^+	4137.2	763.8	32(2)	0.86(6)	$E2$
18^+	4965.9	828.7	26(2)	0.9(1)	$E2$
(20^+)	5875.7	909.8	15(1)		$E2$
(22^+)	6870.2	994.5	9(1)		$E2$
(24^+)	7939.5	1069.3	7.6(9)		$E2$
(26^+)	9063.0	1123.5	4.2(9)		$E2$
(28^+)	10 229.3	1166.3	4.0(9)		$E2$
(30^+)	11 446.0	1216.7	3.5(8)		$E2$
(32^+)	12 726.7	1280.7	3.5(8)		$E2$
(34^+)	14083	1356	<3		$E2$
		Band 2			
$7^{(-)}$	2224.3	846.4	10(1)	0.58(6)	$E1$
$9^{(-)}$	2654.1	429.8	14(1)	0.91(6)	$E2$
		667	<3		$E1$
$11^{(-)}$	3183.3	529.2	13(1)	0.90(8)	$E2$
		523.5	<3		$E1$
(13^-)	3796.2	612.9	13(2)		$E2$
(15^-)	4481.3	685.1	11(2)		$E2$
(17^-)	5232.6	751.3	8(1)		$E2$
(19^-)	6053.0	820.4	6(1)		$E2$
(21^-)	6942.3	889.3	4(1)		$E2$
(23^-)	7888	945	<3		$E2$
		Band 3			
(5^-)	1877.5	1029.0	9.0(8)		$E1$
$7^{(-)}$	2268.7	391	<3		$E2$
		890.8	5.6(7)	0.5(1)	$E1$
		215.6	3.8(7)		$M1/E2$
		340.9	3.5(2)		$E2$
$9^{(-)}$	2751.0	482.3	7(1)	0.98(5)	$E2$
		267.8	3.3(7)		$M1/E2$
$11^{(-)}$	3322.1	571.1	6(1)		$E2$
		314	<3		$M1/E2$
$13^{(-)}$	3955.3	633.2	5(1)		$E2$
$15^{(-)}$	4641.9	686.6	5(1)		$E2$
$17^{(-)}$	5369.0	727.1	4(1)		$E2$
$19^{(-)}$	6165	796	<3		$E2$
$21^{(-)}$	7010	845	<3		$E2$

TABLE I. (*Continued*).

I_i^{π} [a]	E_{level} (keV)	E_γ (keV)[b]	I_γ	DCO[c]	Multipolarity
		Band 4			
(4^-)	1732.6	1307.6	<3		$E1$
(6^-)	2053.2	320.6	6.0(9)		$E2$
		176.1	7.6(9)	0.62(7)	$M1/E2$
(8^-)	2483.5	430.3	9(1)		$E2$
		259.8	4.6(6)		$M1/E2$
		214.2	3.5(6)		$M1/E2$
(10^-)	3009.5	526.0	8(1)		$E2$
		258	<3		$M1/E2$
(12^-)	3589.8	580.3	8(1)		$E2$
(14^-)	4202.0	612.2	7(1)		$E2$
(16^-)	4887.1	685.1	6(1)		$E2$
(18^-)	5646.9	759.8	4.2(1)		$E2$
(20^-)	6490.5	843.6	3.9(1)		$E2$
(22^-)	7382.5	892.0	4(1)		$E2$
(24^-)	8308	925	<3		$E2$
(26^-)	9303	995	<3		$E2$

[a]Spin and parity of the initial state.

[b]Uncertainties in E_γ are 0.2 keV for most transitions, except for relatively weak transitions where they are 0.5 keV.

[c]Relative intensity of the transition calculated with $I_\gamma(291.3) \equiv 100$.

on every combination of γ rays above the 18^+ state. For the transitions below the 18^+ level, DCO ratios were deduced (see Table I) and the $E2$ character of these transitions was confirmed. It should be noted that the DCO ratios for the $E2$ transitions systematically lie under the expected value of 1, although they are mostly within error of this value. This may indicate a small degree of dealignment of the spin (prior to the emission of the γ rays of interest) for which there is no explanation at the present time.

In addition to confirming and extending the previously known ground-state sequence to higher spins, four sidebands were observed. Band 2 is the strongest sideband seen in

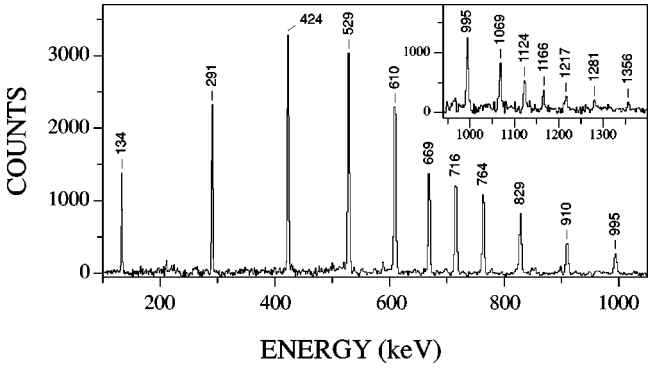

FIG. 2. Spectrum of the ground-state band (band 1) in ^{128}Nd. The spectrum is a result of summing the coincidence spectra generated by double gating on all possible combinations of γ rays above the 18^+ state in the band. The high-energy part of the spectrum is displayed in the inset.

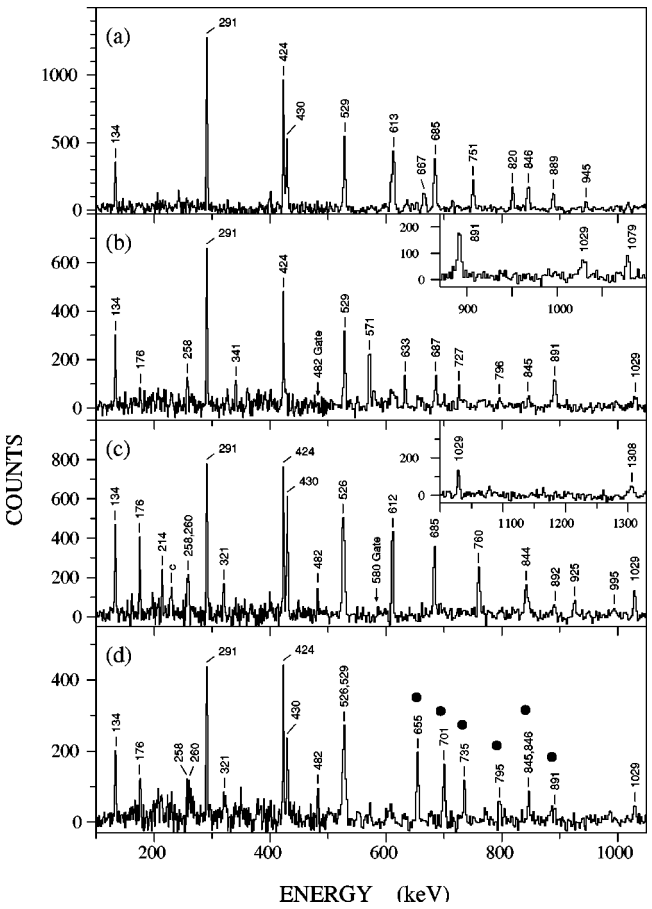

FIG. 3. Spectra of the sidebands in ^{128}Nd. The spectrum of band 2 shown in panel (a) is a result of summing several in-band coincidence double gates. (b) Spectrum of band 3 produced by summing coincidence double gates of the 482.3-keV transition with the lower four transitions of the ground-state band. (c) Spectrum of band 4 produced by summing clean double-gated coincidence spectra of in-band transitions with the 580.3-keV γ ray. The inset shows the linking transitions to the ground-state band. (d) Spectrum of another possible sideband produced in a similar manner as panel (c). In-band transitions are marked with a filled circle. As explained in the text, this band was not incorporated in the level scheme. Peaks denoted by "*c*" refer to contaminant transitions.

^{128}Nd, as indicated in Table I. A representative spectrum of the sequence is displayed in Fig. 3(a). The measured DCO ratio of 0.58(6) for the 846.4 keV linking transition from the state at 2224.3 keV in band 2 to the 8^+ state of band 1 implies a change in spin of one unit of $\hbar$. A $I \rightarrow I-1$ assignment to this γ ray would result in band 2 becoming yrast above the 5232.6-keV state, which contradicts the pattern of the measured intensities for bands 1 and 2 (see Table I). A $I \rightarrow I+1$ assignment for the 846.4-keV γ ray provides a scenario more consistent with the observed intensities. Based on this argument, the 2224.3-keV state is assigned a spin of $I=7$. With this assignment, the sequence is observed up to spin $I=23\hbar$. The absence of $I \rightarrow I-1$ transitions, which would be favored due to the larger γ-ray energy, is discussed below. Although, a firm parity assignment cannot be made for band 2, negative parity is proposed on the basis of the systematics of the lowest sidebands in even-even Nd nuclei [4,11,12]. This assignment also agrees well with the configuration assignment of band 2, as discussed below.

Bands 3 and 4 are found to be interlinked by several weak transitions assumed to be of mixed $M1/E2$ character. Band 3 primarily decays through the 890.8-keV transition to band 1, which has a DCO ratio of 0.5(1). A change of $1\hbar$ is, therefore, associated with this linking transition. Once again, intensity considerations favor a $I \rightarrow I+1$ assignment over a $I \rightarrow I-1$ possibility for this γ ray as the latter would make levels in band 3 approximately 400 keV lower in energy than states with comparable spins in band 2. The smaller intensities of band 3 in comparison with band 2 (see Table I) suggest that band 3 is the more highly excited band. Thus, the state at 2268.7 keV is assigned a spin of $I=7$. Also this state is found to decay to the ground-state band via the 340.9-keV and 1078.9-keV transitions. Negative parity is proposed for bands 3 and 4 based upon configuration assignments discussed in the following section. With this parity, one may note that an $I \rightarrow I-1$ assignment for the 890.8-keV γ ray would suggest an $M2$ multipolarity for the 1307.6-keV transition from the 1732.6-keV state in band 4. γ rays of this multipolarity are not commonly observed in rotational nuclei, therefore lending further credence to the proposed spins. Band 4 also decays into the $I^{\pi}=7^{(-)}$ level of band 2 through the 259.8-keV transition.

A weak sequence was also observed in coincidence with the ground-state band of ^{128}Nd, but definitive linking transitions to other bands could not be established. A representative spectrum is shown in Fig. 3(d), where the in-band transitions are denoted with filled circles. The sequence is in coincidence with transitions below the 8^+ and (10^-) states in bands 1 and 4, respectively. The 655-keV transition was observed to be a doublet in coincidence with band 5, therefore, it may conceivably correspond to a linking transition. However, no other possible linking γ rays could be identified, and a firm placement will have to await another measurement with higher statistics. Spin and parity for this structure are impossible to assign at this time.

IV. ROTATIONAL ALIGNMENTS AND CONFIGURATION ASSIGNMENTS

For a discussion of the ground-state band and of the possible configuration assignments for the sidebands in ^{128}Nd, the rotational alignments of bands 1–4 are presented in Fig. 4. Harris parameters [13] of $\mathcal{J}_0=22\hbar^2/\mathrm{MeV}$ and $\mathcal{J}_1=17\hbar^4/\mathrm{MeV}^3$ were used to subtract the angular momentum of the collective core. CSM calculations [14] were performed using deformation parameters extracted from total Routhian surface (TRS) calculations [15]. The results are displayed in Fig. 5 with the orbital labeling scheme summarized in Table II. The quasiparticle trajectories were labeled in Fig. 5, based on calculated single-particle levels near the Fermi surface, by the same Woods-Saxon potential used for the CSM calculations. This single-particle diagram may be found in Fig. 5 of Ref. [16].

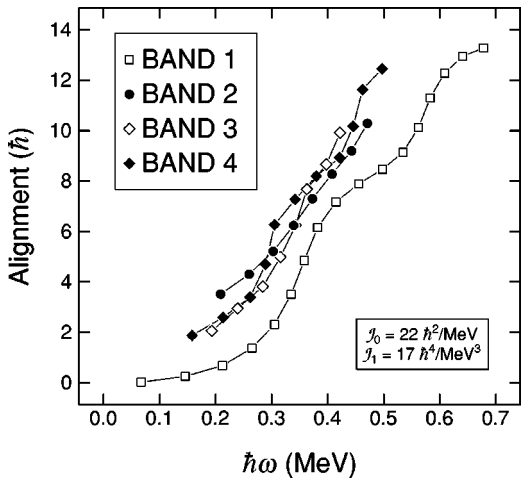

FIG. 4. Experimental alignments versus rotational frequency for bands 1–4 in ^{128}Nd. Harris parameters of $\mathcal{J}_0 = 22\hbar^2/\mathrm{MeV}$ and $\mathcal{J}_1 = 17\hbar^4/\mathrm{MeV}^3$ were used to subtract the angular momentum of the collective core.

A. Band 1

A large alignment gain, at a crossing frequency of $\hbar\omega_c \sim 0.35$ MeV, is observed for band 1. The only nucleons that can align at this low frequency and give such a large increase in alignment are the low-K $h_{11/2}$ protons (not shown in Fig. 5). This proton alignment (E_pF_p) is well documented in the mass-130 region, where the crossing frequency and alignment gain in ^{128}Nd are similar to those observed in nearby nuclei [17]. CSM calculations predict the E_pF_p crossing at $\hbar\omega \sim 0.37$ MeV, in good agreement with the experimental observations. The next indication for a crossing in band 1 is observed at a frequency of ~ 0.57 MeV, as seen in Fig. 4.

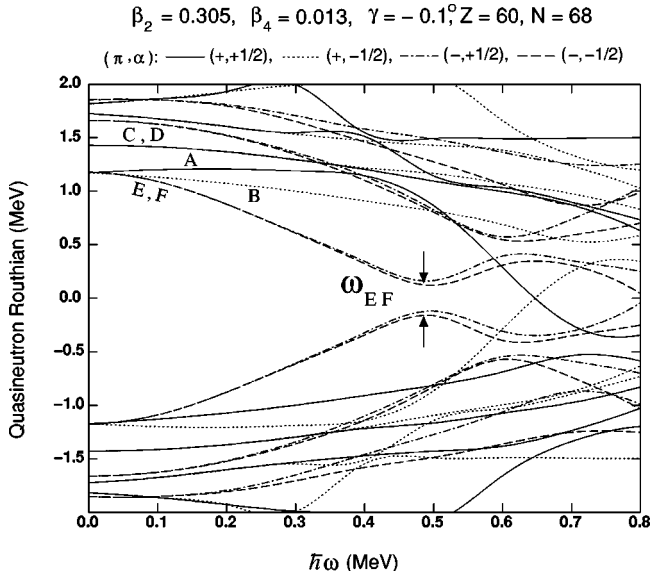

FIG. 5. Cranked shell model calculations for quasineutrons in ^{128}Nd. The deformation parameters (shown at the top of the figure) were determined from TRS calculations [15]. The interpretation of the lines is given at the top of the figure, the orbital labeling scheme can be found in Table II.

An alignment of $h_{11/2}$ quasineutrons (EF) is likely responsible for this crossing. However, the CSM quasineutron diagram shown in Fig. 5 indicates that the EF alignment is calculated to occur near 0.47 MeV. Further discussion of this implied substantial delay in the EF neutron crossing in ^{128}Nd and in neighboring nuclei follows in a later section.

B. Band 2

Band 2 has an initial alignment of approximately $2.5\hbar$ and experiences a significant alignment gain over the frequency range seen in Fig. 4. This gain can presumably be associated with the E_pF_p crossing since the second proton crossing (F_pG_p) is found to occur at a higher frequency of $\hbar\omega \sim 0.42$ MeV in the $\pi h_{11/2}$ band of the $N=68$ isotone $^{127}_{59}$Pr [18]. This $\pi h_{11/2}$ band is also found to constitute the yrast sequence in ^{127}Pr. Therefore, the lowest lying two-quasiproton band in ^{128}Nd would likely have this proton in its configuration, and such a two-quasiparticle configuration would Pauli block the $\pi h_{11/2}$ crossing. Since there is no apparent blocking in band 2, a two-quasineutron configuration is a preferred possibility. From an inspection of the band structures observed in the neighboring odd-N ^{129}Nd [16] nucleus, one can conclude that the neutron orbitals $d_{3/2}/s_{1/2}[411]1/2$ (A,B), $d_{5/2}[402]5/2$ (C,D), $h_{11/2}[523]7/2$ (E,F), and $h_{9/2}/f_{7/2}[541]1/2$ (G,H) (see footnote 1) are all located near the neutron Fermi surface for ^{128}Nd. The band associated with the [523]7/2 state is the most intensely populated structure in ^{129}Nd [16], suggesting that this neutron is a likely constituent of the lowest lying two-quasineutron configuration in ^{128}Nd. Therefore, band 2 has the E neutron in its configuration (the E configuration is systematically found to be energetically favored over its signature partner F). Since E has a signature of $\alpha = -\frac{1}{2}$ and band 2 has been determined to have $\alpha = 1$ (i.e., it is an odd-spin sequence), the second quasineutron must also have negative signature, leaving B, D, and G as possibilities. To reduce the number of possible configurations, one can consider the additivity of alignment for these quasineutrons. The experimental alignment values (in units of $\hbar$) at $\hbar\omega = 0.2$ MeV for the configurations observed in ^{129}Nd are as follows: $A=0.7$, $B=1.3$, $C=0.8$, $D=0.8$, $E=2.1$, $F=2.1$, $G=2.1$, and $H=2.8$. Adding the values for the E and G neutrons would result in a larger alignment ($4.2\hbar$) than that observed for band 2 ($\sim 3.5\hbar$) at $\hbar\omega \sim 0.2$ MeV. In addition, G is the unfavored signature of the [541]1/2 orbital and is highly unlikely to be associated with the lowest sideband in ^{128}Nd. Bands involving the [402]5/2 orbital are normally strongly coupled with little signature splitting. Therefore, if the ED configuration is observed, one would expect to see it coupled with its EC signature partner, which is not the case for band 2. Summing the alignments of the E and B neutrons results in a value close to the experimentally observed alignment of band 2. Large signature splitting is seen for the [411]1/2 band in

[1]For simplicity, G and H are assigned to the [541]1/2 orbital due to the fact that this state was observed in ^{129}Nd. However, the G,H trajectories in Fig. 5 may not correspond to this configuration.

TABLE II. Alphabetic quasiparticle labeling scheme for ^{128}Nd.

Label	$(\pi,\alpha)_n$[a]	Configuration[b]
	Quasineutrons	
A	$(+,+\frac{1}{2})_1$	[411]1/2
B	$(+,-\frac{1}{2})_1$	[411]1/2
C	$(+,+\frac{1}{2})_2$	[402]5/2
D	$(+,-\frac{1}{2})_2$	[402]5/2
E	$(-,-\frac{1}{2})_1$	[523]7/2
F	$(-,+\frac{1}{2})_1$	[523]7/2

[a]Parity (π) and signature (α) of the orbital. The subscript *n* numbers the quasiparticle excitations of a specific signature and parity starting with the lowest in energy at $\hbar\omega=0$ MeV.
[b]Configuration of the orbital at $\hbar\omega=0$ MeV.

^{129}Nd [16], with the $\alpha=-\frac{1}{2}$ signature being favored. Thus, the observed decoupled sequence of band 2 is consistent with the *EB* configuration.

C. Bands 3 and 4

Similar to band 2, large alignment gains are found throughout the observed frequency range of bands 3 and 4. Once again, this is most likely associated with the E_pF_p crossing, and indicates that these structures are built on two-quasineutron excitations. The average of the initial alignments of bands 3 and 4 at $\hbar\omega=0.2$ MeV is $\sim 2.3\hbar$. This is somewhat lower than expected for the *EC* and *ED* configurations ($\sim 2.9\hbar$) at $\hbar\omega\sim 0.2$ MeV (see discussion in Sec. IV B). However, the presence of low-energy $\Delta I=1$ linking transitions between bands 3 and 4 at low spin strongly argues for an interpretation in terms of coupled signature partners. As stated previously, bands involving the [402]5/2 orbital are strongly coupled, and therefore, one should observe both signatures, which is consistent with our experimental findings. From the spins of the levels in band 3, a $\alpha=0$ signature can be inferred and, as a result, this sequence is assigned the *ED* configuration. It then follows that band 4 is assigned the *EC* configuration ($\alpha=1$ signature).

The configurations associated with bands 3 and 4 may well point to a possible explanation for the noticeable absence of $I\rightarrow I-1$ transitions linking these sidebands to the yrast line. The orbitals involved originate from the $h_{11/2}$ and $d_{5/2}$ shells, which are characterized by $\Delta j=\Delta l=3$. Nazarewicz and Tabor [19] suggested that octupole correlations occur when orbitals with these characteristics are present near the Fermi surface. Hence, such correlations are likely to be present in bands 3 and 4. The $d_{5/2}$ and $d_{3/2}/s_{1/2}$ orbitals are found to mix strongly in the ^{128}Pr [20] and ^{129}Nd [16] neighbors and, thus, band 2 may also be affected by these octupole correlations. In the mass-180 region, $I\rightarrow I+1$ linking transitions from sidebands of octupole vibrational character are also found to be favored over the $I\rightarrow I-1$ transitions (see, e.g., Refs. [21–23]). As discussed in Refs. [21,24], the ratio between the intensities of these two types of interband transitions depends delicately on the phase differences arising for transitions with $\Delta K=1$ and $\Delta K=0$ quantum numbers. It is possible that the absence of $I\rightarrow I-1$ transitions in ^{128}Nd is of a similar origin.

V. SYSTEMATICS OF THE $\nu h_{11/2}$ CROSSING IN $A\sim 130$ NUCLEI

Band crossing frequencies are a valuable tool in exploring nuclear properties such as deformation and pairing. The ability to correctly predict various crossings in the rare-earth region has made the cranked shell model a powerful tool for describing observed alignments and associated properties. However, understanding the systematics of the neutron $h_{11/2}$ crossing in nuclei with $A\sim 130$ has been particularly challenging, partially due to the predicted triaxial softness of the heavier nuclei in this mass region [16,25,26]. Therefore, by focusing on the neutron-deficient nuclei near $N=70$ and $Z=60$, which are likely more rigid in their axial deformation [1], one hopes to gain a better understanding about how the alignments depend on the deformation and the location of the Fermi levels. Surprisingly, large deviations have been observed between the experimental crossing frequencies and the predicted CSM values. For instance, Paul *et al.* [27] observed that the experimental $\nu h_{11/2}$ crossing for even-even Ce nuclei ($N=66$–74) occurs at significantly higher frequencies than the predicted CSM values, and reaches a maximum ($\hbar\omega_c>0.69$ MeV) for $N=70$ (^{128}Ce). This crossing value is a $>55\%$ deviation with respect to the CSM predicted value of $\hbar\omega_c\sim 0.44$ MeV. In contrast, CSM calculations of the proton $h_{11/2}$ crossing in even-even, neutron-deficient Ce and Nd nuclei are in excellent agreement with the measured values.

We have extended the systematics of Paul *et al.* [27] for the $\nu h_{11/2}$ crossing to include La, Nd, and odd-odd Pr nuclei. Table III lists the nuclei of interest, the bands in which a $\nu h_{11/2}$ crossing have been observed, the crossing frequency values, and the relevant references for the data. For even-even nuclei the ground-state band was used, while the structures with the lowest excitation, which do not involve a $h_{11/2}$ neutron were chosen in the odd-*A* and odd-odd nuclei. For discussion purposes, the crossing frequencies of the $\nu h_{11/2}$ alignments for all the nuclei listed in Table III are plotted versus the neutron number *N* in Fig. 6.

Several trends can be identified when examining Fig. 6. Starting with the lowest *Z* isotopic chain (La nuclei), a steady increase in crossing frequency with *N* is observed for both odd-*A* and odd-odd La nuclei. Note that the neutron Fermi surface is located increasingly higher in the $\nu h_{11/2}$ shell as *N* increases. Hence, quasiparticles from high-*K* orbitals require more energy to align, and an increase in rotational frequency with *N* is expected. The neutron crossing in $\pi h_{11/2}\nu d_{5/2}$ bands of the odd-odd La nuclei is observed at a noticeably lower frequency as compared with the odd-*A* $\pi h_{11/2}$ bands. Hartley *et al.* [17] suggested that this staggering between the odd-*A* and odd-odd crossing frequencies may be due to a

TABLE III. The experimental neutron $h_{11/2}$ crossing frequency for rotational bands in $^{128-134}$Nd, $^{127-133}$Pr, and $^{126,128-132}$Ce. Except for ^{128}Nd, the experimental data on these nuclei were compiled from sources listed in the last column.

Nucleus	Configuration	Neutron crossing	Reference
^{128}Nd	g.s.b.	0.57 (1)	
^{129}Nd	$\nu d_{5/2}[402]5/2^+$	>0.58	[16]
^{130}Nd	g.s.b.	>0.66	[4]
^{131}Nd	$\nu d_{5/2}[402]5/2^+$	0.48 (2)	[28]
^{132}Nd	g.s.b.	0.50 (3)	[29]
^{133}Nd	$\nu g_{7/2}[404]7/2^+$	0.46 (2)	[30]
^{134}Nd	g.s.b.	>0.62	[12]
^{127}Pr	$\pi h_{11/2}[541]3/2^-$	0.55 (2)	[18]
^{128}Pr	$\pi h_{11/2}[541]3/2^- \otimes \nu d_{5/2}[402]5/2^+$	0.63 (3)	[20]
^{129}Pr	$\pi h_{11/2}[541]3/2^-$	0.66 (0)	[31]
^{130}Pr	$\pi h_{11/2}[541]3/2^- \otimes \nu d_{5/2}[402]5/2^+$	>0.65	[32]
^{131}Pr	$\pi h_{11/2}[541]3/2^-$	0.57 (1)	[33]
^{132}Pr	$\pi h_{11/2}[541]3/2^- \otimes \nu g_{7/2}[404]7/2^+$	>0.53	[34]
^{133}Pr	$\pi_{11/2}[541]3/2^-$	0.52 (1)	[35]
^{126}Ce	g.s.b.	0.50 (1)	[36]
^{128}Ce	g.s.b.	>0.69	[27]
^{129}Ce	$\nu d_{5/2}[402]5/2^+$	>0.59	[37]
^{130}Ce	g.s.b.	0.66 (3)	[38]
^{131}Ce	$\nu g_{7/2}[404]7/2^+$	>0.57	[39]
^{132}Ce	g.s.b.	0.62 (0)	[40]
^{125}La	$\pi h_{11/2}[550]1/2^-$	0.47 (2)	[17]
^{126}La	$\pi h_{11/2}[550]1/2^- \otimes \nu d_{5/2}[402]5/2^+$	0.40 (2)	[41]
^{127}La	$\pi h_{11/2}[550]1/2^-$	0.50 (2)	[42]
^{128}La	$\pi h_{11/2}[550]1/2^- \otimes \nu d_{5/2}[402]5/2^+$	0.43 (2)	[43]
^{129}La	$\pi h_{11/2}[550]1/2^-$	0.57 (2)	[44]
^{130}La	$\pi h_{11/2}[550]1/2^- \otimes \nu g_{7/2}[404]7/2^+$	0.46 (2)	[45]
^{131}La	$\pi h_{11/2}[550]1/2^-$	0.54 (2)	[46]

reduced pairing field caused by the blocking of a neutron orbital in odd-N versus even-N nuclei. However, it is also possible that the oblate driving $h_{11/2}$ neutrons couple with the oblate driving $d_{5/2}$ neutron. This coupling could result in a shape change and, thus, influence the crossing frequency.

In contrast to La nuclei, the other isotopic chains do not exhibit a consistent systematic behavior. In most of the Ce nuclei, the $\nu h_{11/2}$ crossing is delayed to such a large extent that it is not seen up to the highest frequencies accessible experimentally. Thus, only lower limits are shown in Fig. 6, and definitive trends cannot be extracted. However, significant increases in the crossing frequencies of the Ce nuclei are observed over those found for La. Starting from $N=68$, the crossing frequency in the praseodymium nuclei increases with N, peaks at $N=70$, and then decreases for higher N, a trend opposite to that in La. The $N=71$–73 Nd nuclei exhibit $\nu h_{11/2}$ crossing frequencies at approximately the values predicted by the CSM, but a sharp jump in the frequency is seen at $N=70$, with decreasing values at lower N. These trends suggest that the crossing is maximally delayed near $N=70$ for the $Z=58$–60 nuclei.

Cranked shell model calculations were performed for each of the nuclei listed in Table III. Deformation (quadrupole β_2, hexadecapole β_4, and triaxial γ) and pairing (Δ) parameters were first determined from TRS calculations. For a given isotopic chain, it was found that the CSM predicts a relatively constant value of the crossing frequency for all the nuclei over the neutron range of interest. The average calculated values for the $\nu h_{11/2}$ crossing were $\sim$0.42 MeV, $\sim$0.42 MeV, $\sim$0.44 MeV, and $\sim$0.48 MeV for La, Ce, Pr, and Nd, respectively. Good agreement is generally seen for the light La and heavy Nd nuclei, but large discrepancies are found for all other nuclei. In addition, the calculations fail to reproduce the peak in crossing frequency at $N=70$.

In order to determine if deformation or pairing (as treated in the CSM) could be responsible for these delays, these parameters were varied in a systematic approach. Although Paul *et al.* [27] discussed the effect of quadrupole deformation on this crossing frequency within the cranking model,

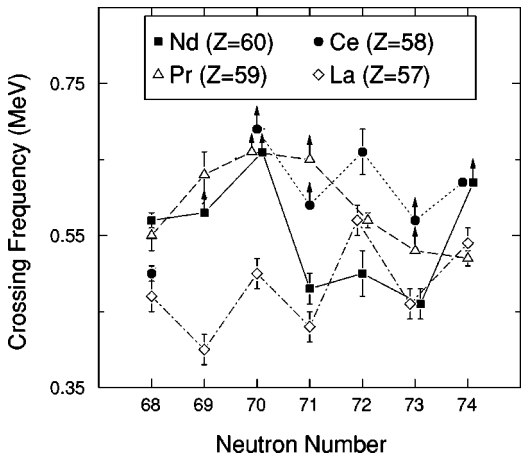

FIG. 6. Experimental neutron $h_{11/2}$ crossing frequencies for lanthanum ($Z=57$), cerium ($Z=58$), praseodymium ($Z=59$), and neodymium ($Z=60$) nuclei. Arrows indicate that the neutron $h_{11/2}$ crossing was not observed up to the highest known frequency, therefore, only a lower limit can be displayed.

we have included a variation of hexadecapole and triaxial deformations, as well as pairing in our study. In each calculation, three of the CSM input parameters were fixed at a given value and the fourth was varied in small steps. This procedure was repeated many times for all the relevant input parameters over the following parametric ranges: $0.24<\beta_2<0.48$, $-30°<\gamma<+30°$, $-0.1<\beta_4<0.1$, and $0.6<\Delta_n<1.4$ MeV. In this manner, numerous combinations of β_2, β_4, γ, and Δ_n were inspected. For practical purposes, the calculations focused on ^{128}Ce as the largest difference between experimental and predicted crossing frequencies occurs for this case (see Table III). The calculations show a smooth increasing trend of crossing frequency with increasing β_2 and Δ_n with maximum achievable values at $\beta_4=0$ and $\gamma=0°$. We were able to reproduce a large experimental crossing frequency in ^{128}Ce only with the unrealistically large value of $\beta_2\sim0.46$. Thus, we are in agreement with Paul *et al.* [27] that the CSM is insufficient for describing this anomaly.

A comparison of the delayed crossings observed in the Ce-Nd region with those found in other mass regions indicate that the $\nu h_{11/2}$ alignments have some of the largest delays currently known. Delays in the $\nu i_{13/2}$ alignment are observed in the proton [541]1/2 configurations found in the $A\sim170$ region (see Ref. [47], and references therein). However, the delays are smaller ($\sim$20–30 % larger than expected) as compared with the $\nu h_{11/2}$ crossing near $N=70$ in the $A\sim130$ region ($\sim$40–55 % larger than expected). Explanations for the delayed crossing in the $h_{9/2}$ bands are configuration dependent, which include enhanced deformations and residual proton-neutron interactions [47,48]. Although this reasoning works well for the heavier nuclei, a more comprehensive description is necessary for the $A\sim130$ nuclei as the delay appears in several configurations (see Table III) and, thus, is a general feature of the region. It is also interesting to note that significant delayed crossings in ground-state sequences are rare. In fact, the only other instances where this occurs are the $N=Z$, $A\sim80$ nuclei [49,50] and in a few Pu nuclei [51]. The $g_{9/2}$ alignment is found to be delayed by $\leqslant$30% for only the $N=Z$ nuclei of $_{36}$Kr, $_{38}$Sr, $_{40}$Zr, $_{42}$Mo, and $_{44}$Ru. Once again, these delays are less than those observed in the $A\sim130$ region and are possibly explained by effects from n-p pairing. Since $N\geqslant Z+8$ for the nuclei considered in this work, n-p pairing can be ruled out for the delay in the $\nu h_{11/2}$ crossing. A possible transition from octupole vibration to octupole deformation has been suggested for the delays ($\geqslant$15%) in the Pu nuclei [51]. However, stable octupole deformation is not expected in the well-deformed light ($A\approx130$) region, although octupole vibrations may exist, as discussed in the preceding section. Thus, the magnitude and the general occurrence for the delayed $\nu h_{11/2}$ alignments is distinctive in comparison with other nuclei.

One may postulate that perhaps the CSM is incorrectly calculating the placement of the $h_{11/2}$ shell. If the Fermi surfaces were located closer to higher K orbitals, larger crossing frequencies would be expected, as discussed above for the La nuclei. However, experimental observations in neighboring odd-N nuclei, such as ^{129,131}Nd [16,28], suggest that the Woods-Saxon potential is correctly predicting mid-K $h_{11/2}$ orbitals near $N=70$. In addition, this argument would fail to explain the peak in crossing frequency at $N=70$. Instead, one would expect steadily increasing crossing frequencies as N increases, similar to that observed in the La nuclei shown in Fig. 6.

The large magnitude of the delay may suggest that more than one force is responsible for this phenomenon. As suggested by Paul *et al.* [27], quadrupole pairing may play a role, as QQ pairing is not incorporated into CSM calculations. Indeed, projected shell model calculations have indicated that a delay in crossing frequency may occur with the inclusion of quadrupole pairing [52]. The cranking calculations also treat deformation and pairing in a static manner (i.e., they are assumed to be the same both before and after the crossing), whereas these parameters may alter significantly due to the successive $\pi h_{11/2}$ and $\nu h_{11/2}$ alignments. Predictions from models that incorporate a self-consistent treatment of deformation and pairing may be more suitable for understanding the delay [27]. However, an inherent difficulty is present due to the fact that the $\nu h_{11/2}$ crossing is the second alignment observed in these rotational bands. In the aforementioned delays of the $A\sim80$, 170, and 240 regions, the delayed crossings normally occur for the first alignments, which are generally more easily treated than higher frequency crossings. Therefore, the substantial delay of the $\nu h_{11/2}$ crossing appears to be a complex and intriguing problem that requires further theoretical work.

VI. SUMMARY

This investigation of high-spin states in ^{128}Nd has resulted in the extension of the previously known ground-state band up to higher spins such that the $\nu h_{11/2}$ crossing was observed. Four sidebands were identified and assigned configurations. The systematics for the $\nu h_{11/2}$ crossings in the neutron-deficient Nd, Pr, Ce, and La nuclei were presented.

The trends show large delays in the $\nu h_{11/2}$ crossing in many of the nuclei surveyed. Indeed, the delays in the crossing frequencies are some of the largest ever observed, and appear to peak at $N=70$. Cranked shell model calculations could not reproduce the high frequency crossing or the peak at $N=70$. However, it is possible that other effects, such as quadrupole pairing and/or deformation changes between the two- and four-quasiparticle bands, may influence the crossing frequency. More theoretical work is clearly necessary to fully understand this complicated anomaly.

ACKNOWLEDGMENTS

Special thanks to D. C. Radford and H. Q. Jin for their software support. The authors wish to thank the ANL operations staff at Gammasphere. Special thanks also to J. Greene for target preparation and use. This work was funded by the U.S. Department of Energy through Contracts No. DE-FG02-96ER40983 (University of Tennessee), W-31-109-ENG-38 (Argonne National Laboratory), and DE-FG05-88ER40406 (Washington University).

[1] P. Möller and J.R. Nix, At. Data Nucl. Data Tables **59**, 185 (1995).
[2] B.H. Smith, L.L. Riedinger, H.Q. Jin, W. Reviol, W. Satula, A. Galindo-Uribarri, D.G. Sarantites, J.N. Wilson, D. LaFosse, and S.M. Mullins, Phys. Lett. B **443**, 89 (1998).
[3] A. Galindo-Uribarri, Rev. Mex. Fis. **45**, 55 (1999).
[4] D.J. Hartley *et al.*, Phys. Rev. C **63**, 024316 (2001).
[5] C.M. Petrache *et al.*, Eur. Phys. J. A **12**, 139 (2001).
[6] R. Janssens and F. Stephens, Nucl. Phys. News **6**, 9 (1996).
[7] D.G. Sarantites, P.-F. Hua, M. Devlin, L.G. Sobotka, J. Elson, J.T. Hood, D.R. LaFosse, J.E. Sarantites, and M.R. Maier, Nucl. Instrum. Methods Phys. Res. A **381**, 418 (1996).
[8] D.C. Radford, Nucl. Instrum. Methods Phys. Res. A **361**, 297 (1995).
[9] C.J. Lister *et al.*, Phys. Rev. Lett. **55**, 810 (1985).
[10] R. Moscrop, M. Campbell, W. Gelletly, L. Goettig, C.J. Lister, and B.J. Varley, Nucl. Phys. **A499**, 565 (1989).
[11] C.M. Petrache *et al.*, Phys. Lett. B **387**, 31 (1996).
[12] R. Wadsworth, S.M. Mullins, J.R. Hughes, P.J. Nolan, A. Kirwan, P.J. Bishop, I. Jenkins, M.J. Godfrey, and D.J. Thornley, J. Phys. G **15**, L47 (1989).
[13] S.M. Harris, Phys. Rev. **138**, 509 (1965).
[14] R. Bengtsson and S. Frauendorf, Nucl. Phys. **A327**, 139 (1979); **A314**, 27 (1979).
[15] R. Wyss, J. Nyberg, A. Johnson, R. Bengtsson, and W. Nazarewicz, Phys. Lett. B **215**, 211 (1988).
[16] O. Zeidan *et al.*, Phys. Rev. C **65**, 024303 (2002).
[17] D.J. Hartley *et al.*, Phys. Rev. C **60**, 014308 (1999).
[18] S.M. Mullins *et al.*, Phys. Rev. C **58**, R2626 (1998).
[19] W. Nazarewicz and S.L. Tabor, Phys. Rev. C **45**, 2226 (1992).
[20] D.J. Hartley *et al.*, Phys. Rev. C **65**, 044329 (2002).
[21] G.D. Dracoulis, C. Fahlander, and M.P. Fewell, Nucl. Phys. **A383**, 119 (1982).
[22] M.J.A. De Voight, R. Kaczarowski, H.J. Riezebos, R.F. Noorman, J.C. Bacelar, M.A. Delephanque, R.M. Diamond, F.S. Stephens, J. Sauvage, and R. Roussíere, Nucl. Phys. **A507**, 472 (1990).
[23] F.G. Kondev *et al.*, Phys. Rev. C **61**, 044323 (2000).
[24] F.W.N. de Boer, P. Koldewijn, R. Beetz, J.L. Maarleveld, J. Konijn, R. Janssens, and J. Vervier, Nucl. Phys. **A290**, 173 (1977).
[25] A. Granderath, P. F Mantica, R. Bengtsson, R. Wyss, P. von Brentano, A. Gelberg, and F. Seiffert, Nucl. Phys. **A597**, 427 (1996).
[26] N. Xu, Jing-ye Zhang, Y. Liang, R. Ma, E.S. Paul, and D.B. Fossan, Phys. Rev. C **42**, 1394 (1990).
[27] E.S. Paul *et al.*, Nucl. Phys. **A676**, 32 (2000).
[28] D.J. Hartley *et al.*, Phys. Rev. C **61**, 044328 (2000).
[29] R. Wadsworth, J.M. O'Donnel, D.L. Watson, P.J. Nolan, A. Kirwan, P.J. Bishop, M.J. Godfrey, D.J. Thornley, and D.J.G. Love, J. Phys. G **14**, 239 (1988).
[30] D. Bazzacco *et al.*, Phys. Rev. C **58**, 2002 (1998).
[31] A. Galindo-Uribarri *et al.* (unpublished).
[32] B.H. Smith, Ph.D. thesis, University of Tennessee, 1998.
[33] A. Galindo-Uribarri *et al.*, Phys. Rev. C **50**, R2655 (1994).
[34] C.M. Petrache, S. Brant, D. Bazzacco, G. Falconi, E. Farnea, S. Lunardi, V. Paar, Zs. Podolyák, R. Venturelli, and D. Vretenar, Nucl. Phys. **A635**, 361 (1998).
[35] E.S. Paul *et al.*, Nucl. Phys. **A690**, 341 (2001).
[36] A.N. Wilson *et al.*, Phys. Rev. C **63**, 054307 (2001).
[37] R. Aryaeinejad, D.J.G. Love, A.H. Nelson, P.J. Nolan, P.J. Smith, D.M. Todd, and P.J. Twin, J. Phys. G **10**, 955 (1984).
[38] A.T. Semple *et al.*, J. Phys. G **24**, 1125 (1998).
[39] M. Palacz, Z. Sujkowski, J. Nyberg, J. Bacelar, J. Jongman, W. Urban, W. Hesselink, J. Nasser, A. Plompen, and R. Wyss, Z. Phys. A **338**, 467 (1991).
[40] E.S. Paul *et al.*, Nucl. Phys. **A619**, 177 (1997).
[41] J. Timár *et al.*, Eur. Phys. J. A **7**, 7 (2000).
[42] K. Starosta *et al.*, Phys. Rev. C **53**, 137 (1996).
[43] M.J. Godfrey *et al.*, J. Phys. G **15**, 487 (1989).
[44] Y. He *et al.*, J. Phys. G **18**, 99 (1992).
[45] O. Zeidan *et al.* (unpublished).
[46] E.S. Paul *et al.*, Phys. Rev. Lett. **58**, 984 (1987).
[47] H.J. Jensen *et al.*, Nucl. Phys. **A695**, 3 (2001).
[48] W. Reviol *et al.*, Phys. Rev. C **59**, 1351 (1999).
[49] S.M. Fischer *et al.*, Phys. Rev. Lett. **87**, 132501 (2001).
[50] N. Mărginean *et al.*, Phys. Rev. C **65**, 051303(R) (2002).
[51] I. Wiedenhöver *et al.*, Phys. Rev. Lett. **83**, 2143 (1999).
[52] Y. Sun, S.X. Wen, and D.H. Feng, Phys. Rev. Lett. **72**, 3483 (1994).